

# Nonlinear automatic control of autonomous lawn mower

**Hannah Dysenius**

Master of Science Thesis in Electrical Engineering

**Nonlinear automatic control of autonomous lawn mower**

Hannah Dysenius

LiTH-ISY-EX-16/4966-SE

Supervisor: **Måns Klingspor**  
ISY, Linköpings universitet  
**Björn Mannefred & Mikaela Åhlén**  
Husqvarna AB

Examiner: **Professor Anders Hansson**  
ISY, Linköpings universitet

*Division of Automatic Control  
Department of Electrical Engineering  
Linköping University  
SE-581 83 Linköping, Sweden*

Copyright © 2016 Hannah Dysenius

## Sammanfattning

Detta examensarbete innehåller modellering och olinjär reglering av en autonom gräsklippare. Fordonet ska kunna följa en magnetslinga nedgrävd i gräsmattan på ett godtyckligt avstånd, inklusive gränslände, med hjälp av endast en magnetometersensor.

Utifrån de fysiska egenskaperna som gräsklipparen besitter har en enhjuling modell härletts för att beskriva klipparen. Modellen gäller då fordonet inte slirar. Denna modell är baserad på tidigare arbeten och är inte ny för detta examensarbete.

Två olika reglerstrategier har använts i detta examensarbete. Den ena bygger på *exakt linjärisering* där en återkoppling har införts med hjälp av en LQ-regulator. Den andra strategin som använts är *linjärisering kring en jämviktspunkt* även denna med LQ-reglering som återkoppling.

Då inte alla tillstånd som används i systemmodellen kan mätas har en observatör tagits fram. Denna observatör är framtagen från modellen *linjärisering kring en jämviktspunkt*. Observatören som har använts är ett Kalmanfilter.

Svårigheten med detta examensarbete har varit att det har funnits väldigt lite information för regulatorn att styra på. Den enda insignalen till systemet är en mätning från en magnetometer. Magnetfältets olinjära beteende gör det svårt att beräkna avståndet till slingan. Detta tillsammans med mätbruset gör att precisionen på regleringen begränsas.

Slutsatsen för detta examensarbete är att det går att navigera och följa slingan bra på ett avstånd större än 0.3 [m] från slingan, dock med överslängar vid skarpa svängar. Om roboten ska följa slingan närmare, blir dess beteende mer slingrande över slingan. Anledningen till att precisionen inte har kunnat förbättras är att mätningarna av magnetfältet är brusiga, att ett uppmätt värde på magnetfältstyrkan ger två olika avstånd och att svårigheten att avgöra det rätta avståndet ökar med minskande avstånd till slingan.



## Abstract

This master thesis contains modeling and nonlinear automatic control of an autonomous lawn mower. The vehicle shall be able to follow a magnetic field loop buried in the lawn on an arbitrary distance, including straddling.

A unicycle model of the lawn mower has been derived based on previous work. The model holds for the assumption of non slip environment.

Two different control strategies have been implemented and evaluated in this thesis. One is based on *feedback linearization* and with the feedback gain estimated using an LQ-controller. The other strategy is based on *linearization at an equilibrium point* and also with the use of an LQ-controller.

The only state that can be measured is the distance to the magnetic loop. In order to estimate the other states, an observer has been implemented using the *linearized in an equilibrium point* model and a Kalman filter.

The navigation of the autonomous lawn mower is performed using a magnetic loop buried in the lawn. The non-linearity of the magnetic field causes difficulties when estimating the distance to the loop. One magnetic field strength corresponds to two distances to the magnetic loop. The nature of the magnetic field and the measurement noise causes the precision of the controller to be limited.

The conclusion of this master thesis is that it is possible to navigate and follow the magnetic loop at a distance greater than 0.3 [m], but with overshoots during sharp turns. If the reference distance is smaller than that, the behavior of the robot will be oscillating when following the loop. The limitations of the controller performance is due to the lack of information which can be extracted from the measurements of the magnetic field.



## Acknowledgments

First of all I would like to thank Husqvarna AB for the opportunity to perform this master thesis. The supervisor at Husqvarna, Björn Mannefred, has been very helpful and supportive and I am very grateful for that.

I would also like to thank my examiner, professor Anders Hansson, and my supervisor, Måns Klingspor, for all the help and time that they have given me during this thesis. They have always been available for discussions about new control strategies and how to solve problems which has emerged along the way.

I would also like to thank my friends and family for their unconditional love and support, you mean the world to me.

*Linköping, May 2016  
Hannah Dysenius*





---

# Contents

<b>Notation</b>	<b>xi</b>
<b>1 Introduction</b>	<b>1</b>
1.1 Background . . . . .	1
1.2 Problem formulation . . . . .	2
1.3 Related work . . . . .	2
1.4 Method . . . . .	3
1.5 Limitations . . . . .	3
1.6 Outline . . . . .	4
<b>2 Preliminaries</b>	<b>5</b>
2.1 Feedback Linearization of nonlinear model . . . . .	5
2.2 Lyapunov stability function . . . . .	7
2.3 Linear Quadratic Controller . . . . .	7
2.4 Linear observer . . . . .	8
2.4.1 Kalman filter . . . . .	8
2.5 Jacobian Linearization, equilibrium points . . . . .	9
2.6 Constrained motion . . . . .	9
<b>3 Robot description</b>	<b>11</b>
3.0.1 Hardware description . . . . .	11
3.0.2 Measurement system . . . . .	12
<b>4 Modeling</b>	<b>13</b>
4.1 System model . . . . .	13
4.2 Feedback linearization . . . . .	16
4.2.1 Lyapunov analysis . . . . .	17
4.3 Linearization in the equilibrium point . . . . .	18
4.4 Discretization of the time-continuous model . . . . .	18
<b>5 Magnetic field navigation</b>	<b>21</b>
5.1 Biot - Savart Law . . . . .	21
5.2 Distance from the magnetic loop to vehicle . . . . .	22

---

5.3	Measured magnetic field . . . . .	23
5.3.1	Distance to the magnetic loop using <i>trend-equations</i> . . . . .	24
5.3.2	Distance to the magnetic loop using <i>look-up table</i> . . . . .	25
<b>6</b>	<b>Results</b>	<b>29</b>
6.1	Results from simulations i Simulink . . . . .	30
6.2	Results from Gazebo simulations . . . . .	34
6.3	Hardware - Husqvarna Automower 330X . . . . .	35
6.3.1	Look-up table . . . . .	35
6.3.2	Trend-function . . . . .	40
<b>7</b>	<b>Conclusions</b>	<b>41</b>
7.1	Conslusions . . . . .	41
7.2	Future work . . . . .	42
<b>A</b>	<b>Appendix A</b>	<b>45</b>
	<b>Bibliography</b>	<b>47</b>

---

# Notation

## SYMBOLS

Symbol	Meaning
$v$	Average velocity
$T$	Sampling time
$\mu_0$	Vacuum permeability
$\mathbf{a}_R$	Unit vector from source point to field point
$\mathbf{a}_r$	Unit vector in the r-direction when using cylinder coordinates
$\mathbf{a}_z$	Unit vector in the z-direction when using cylinder coordinates
$\mathbf{a}_\Phi$	Unit vector in the $\Phi$ -direction when using cylinder coordinates
$\sigma$	Standard deviation

## ACRONYMS

Acronyms	Meaning
ALM	Autonomous Lawn Mower
LQ	Linear Quadratic controller
ROS	Robot Operating System
GPS	Global Positioning System
PID	Proportional Integrative and Derivative
MPC	Model Predictive Control



# 1

---

## Introduction

To be able to construct a unmanned autonomous lawn mower (ALM) one must take into consideration the difficulties of navigating outdoors and the life-span of the hardware.

The navigation outside is one of the most difficult problems to solve in order for the lawn mower to yield satisfying results when mowing the lawn. The accuracy of a GPS is not enough. To solve the navigation the lawn mower used in this thesis navigates using magnetic loops buried in the lawn.

This master's thesis has been developed in cooperation with Husqvarna AB. The thesis consists of modeling and controlling a lawn mower model Husqvarna A330X. The controller is tested both by simulation and using real hardware.

This introductory chapter is a description of the underlying background, related work and the purpose of this master thesis.

### 1.1 Background

The interest and demand of ALMs has increased in recent years as the technique and performance of ALMs have improved. The environment that the robot is set to be operating in requires high standards in both the navigation of the vehicle and in the quality of the hardware used.

The ALM used in this master thesis navigates around the lawn and back to the charging station by using magnetic loops buried in the lawn. The ALM shall then be able to follow the loop at different distances, including straddling. The difficulties that occur when navigating using the magnetic loop is the non-linear

behavior of the magnetic field. On one side of the magnetic loop the value will be positive and when crossing the loop the value will be negative, and close to the magnetic loop the value changes rapidly. Additionally one magnetic field strength will correspond to two different distances to the magnetic loop. When estimating the distance to the loop this will be problematic. This is currently solved by using two magnetic sensors and a PID-controller.

## 1.2 Problem formulation

The task of this master thesis is to model the ALM and to find a controller which can control the ALM by the use of only one magnetic field sensor. The vehicle shall be able to follow the magnetic loop at an arbitrary distance, including straddling. This is a challenge due to the non-linear behavior of the magnetic field strength, and the fact that one magnetic field strength can correspond to two different distances.

The model shall be implemented and simulated using Gazebo<sup>1</sup> and then tested on the Robot Operating System (ROS) enabled lawn mower, Husqvarna Automower 330X.

## 1.3 Related work

The path-following control of mobile robots are widely encountered. The model used in this thesis in the context of feedback control was presented by Alessandor De luca, Giuseppe Oriolo and Claude Samson in [12] and [3]. The method to project the global coordinate system to a curvature in order to follow a trajectory has been treated in [8].

Much research effort has been oriented to solving the problem of motion under nonholonomic constraints using the kinematic model of a mobile robot. One approach to this problem is defining the path-following errors with the Serret-Frenet method [4] where the control design is then usually based on Lyapunov's backstepping and direct methods. Another method is to interpret the path-following errors between the real robot and a virtual robot that follows a reference path [1]. Another method to solve the problem is to convert the path-following problem into an input-output feedback linearization problem using a transverse feedback linearization method [9], [10], [11].

---

<sup>1</sup>A simulation environment designed to be used with ROS-enabled systems. More information can be found at <http://gazebosim.org/>

## 1.4 Method

The methodology of this thesis is presented below:

- Modeling of the system
- Software implementation of model and controllers
- Software simulation
- Testing
- Evaluation
- Hardware implementation and validation on the real system
- Comparison between controllers on the real system

Using the literature study, two models of the system have been produced along with two different control structures. Initially the models and controllers were tested in simulations, both in the simulation environment Simulink and using Gazebo. When satisfying results were accomplished in simulations the models and controllers were tested on real hardware.

The controller structures used in this thesis were based on two different models, *feedback linearization* and *linearization at an equilibrium point*. The feedback gain in both of these control structures were estimated using an LQ-controller. The LQ-controller was estimated using the linearization in an equilibrium point model.

The lack of measurements result in the need of estimating the states. For this an observer has been implemented. The observer is based on the linearized at an equilibrium point model and a Kalman filter.

## 1.5 Limitations

This thesis stretches over a limited period of time, hence there is only room to investigate a few different controllers and models of the system. This time limit might also affect the tuning possibilities of the controllers. There might therefore exist a set of parameters for the controllers presented in this thesis that slightly enhances the performance of the lawn mower.

Due to the complexity of the magnetic loop, the case where the magnetic loop is straight and not curved will be the main problem to solve. The model is designed for a non-curved magnetic loop, but the closed loop makes it possible to follow the loop in curves that are larger than 90 degrees.

The currently existing lawn mower model Husqvarna A330x is the hardware used in this thesis. The simulations are carried out in Simulink and in the ROS enabled simulation environment Gazebo. When simulating using Gazebo an already implemented simulation model of the lawn mower is used.

## 1.6 Outline

The outline of this master thesis is as follows:

- Chapter 2 contains an introduction for the reader of the basic theory that this master thesis will cover.
- Chapter 3 is a short description of the robot used in this thesis.
- Chapter 4 contains a description of the model, and the control strategies used in this master thesis.
- Chapter 5 contains a description of the magnetic field and from using the magnetic field strength and Biot-Savarts law the distance to the magnetic loop can be estimated.
- Chapter 6 contains the results reached in this master thesis.
- Chapter 7 contains a description of the conclusions of this thesis, along with what future work that might be of value to investigate further.



# 2

---

## Preliminaries

This chapter is intended to present the basic knowledge about the areas and sections which this thesis will cover.

### 2.1 Feedback Linearization of nonlinear model

When treating nonlinearities in different applications a common approach is to design a inner feedback to reduce the nonlinear characteristics.

The input-output relationship of a time-invariant nonlinear system can be written on the form shown in (2.1). Here,  $x$  denotes the states,  $u$  the input and  $y$  denotes the output of the system, [6].

$$\begin{aligned}\dot{x} &= F(x, u) = f(x) + g(x)u \\ y &= h(x)\end{aligned}\tag{2.1}$$

For a system with the relative degree  $v$ , described in [5], the following yields:

$$y^{(v)} = L_f^v h + u L_g L_f^{v-1} h, \quad L_g L_f^{v-1} h \neq 0\tag{2.2}$$

where

$$L_f = f_1 \frac{d}{dx_1} + \dots + f_n \frac{d}{dx_n}, \quad L_g = g_1 \frac{d}{dx_1} + \dots + g_n \frac{d}{dx_n}.\tag{2.3}$$

If the input described in (2.4) is used in (2.2) the result will be (2.5), which is a linear system from reference signal to output.

$$u = \frac{1}{L_g L_f^{v-1} h} (r - L_f^v h) \quad (2.4)$$

$$y^{(v)} = r \quad (2.5)$$

With the following variable substitution:

$$z_1 = y, \quad z_2 = \dot{y}, \quad \dots \quad z_v = y^{(v-1)} \quad (2.6)$$

the system can be described as:

$$\begin{aligned} \dot{z}_1 &= z_2 \\ \dot{z}_2 &= z_3 \\ &\vdots \\ \dot{z}_v &= \xi(z) + u\eta(z) \\ \dot{z}_{v+1} &= \phi(z, u) \\ &\vdots \\ \dot{z}_n &= \psi_{n-v}(z, u) \\ y &= z_1 \end{aligned} \quad (2.7)$$

The control signal is then chosen as:

$$u = (r - \xi)/\eta$$

This will then result in:

$$\begin{aligned} \dot{z}_1 &= z_2 \\ \dot{z}_2 &= z_3 \\ &\vdots \\ \dot{z}_v &= r \\ \dot{z}_{v+1} &= \phi(z, (r - \xi)/\eta) \\ &\vdots \\ \dot{z}_n &= \psi_{n-v}(z, (r - \xi)/\eta) \\ y &= z_1 \end{aligned} \quad (2.8)$$

And the system can be written as:

$$\begin{aligned} \dot{z} &= Az + Bu \\ y &= Cz \end{aligned} \quad (2.9)$$

The system presented in (2.8) and (2.9) is exact linearized.

## 2.2 Lyapunov stability function

To study the asymptotic stability behavior of a dynamic system, one commonly used method is the Lyapunov stability theory. A equilibrium point  $x_0$  to the system  $\dot{x} = f(x)$  is globally asymptotically stable if a function  $V$  can be found that satisfies the conditions in (2.10) - (2.12) below, [5].

$$V(x_0) = 0; \quad V(x) > 0, x \neq x_0; \quad (2.10)$$

$$\frac{d}{dt} V(x(t)) = V_x(x(t))f(x(t)) < 0, \quad x \neq x_0 \quad (2.11)$$

$$V(x) \rightarrow \infty, |x| \rightarrow \infty \quad (2.12)$$

## 2.3 Linear Quadratic Controller

Given the linear system (2.9) a Linear Quadratic controller (LQ) can be used to stabilize an unstable system and control it to follow a given reference signal. An LQ-controller is designed by choosing an state feedback gain  $L$  that minimizes the cost function shown in Equation 2.13, [5].

$$\min_u J = \min_u \int_0^{\infty} (z^T Q_1 z + u^T Q_2 u) dt \quad (2.13)$$

where  $Q_1$  and  $Q_2$  are positive, semi-definite weight matrices,  $z$  are the controller variable. Matrices  $Q_1$  and  $Q_2$  are typically chosen to be diagonal. The feedback gain is estimated in Equation 2.14

$$L = Q_2^{-1} B^T S \quad (2.14)$$

where  $S$  is the solution to the Riccati equation shown in (2.15).

$$A^T S + SA + Q_1 - SBQ_2^{-1} S^T B^T = 0 \quad (2.15)$$

Using  $L$  in (2.14) the controller is given by:

$$u = L_r r - Lz \quad (2.16)$$

where  $r$  is the reference signal and  $L_r$  is chosen so that the static gain is 1.

For the special case where there is only one input, the matrix  $Q_2$  is a scalar. As a result, a modification of the cost function can be made, see (2.17)

$$\min_u J = \min_u \int_0^{\infty} (z^T Qz + u^2) dt \quad (2.17)$$

where  $Q = \frac{Q_1}{Q_2}$ .

The matrix  $S$  is the positive semi-definite solution to Equation 2.18a below.

$$Q + A^T S + SA - SBB^T S = 0 \quad (2.18a)$$

$$L = B^T S \quad (2.18b)$$

$$u = L_r r - Lz \quad (2.18c)$$

The signal  $r$  is the desired reference signal.

## 2.4 Linear observer

In the case where all states cannot be measured, an observer can be used to reconstruct these states. Using the linear system described in Equation 2.9 a linear observer can be designed.

If  $z$  denotes the true states and  $\hat{z}$  denotes the estimated states, the observer can be written according to (2.19) below.

$$\dot{\hat{z}} = A\hat{z} + Bu + K(y - C\hat{z}) \quad (2.19)$$

where  $K$  is a  $n$ -dimensional vector if the system only has one output.

The speed of the observer is affected by the choice of  $K$ . If the system is observable then  $K$  can be chosen so that  $A - KC$  has arbitrary eigenvalues.

### 2.4.1 Kalman filter

The choice of  $K$  is a compromise between the speed of reconstruction and the sensitivity for measurement noise. If white noise is added to the model 2.9 the system will result in Equation 2.20, [5].

$$\begin{aligned} \dot{z} &= Az + Bu + Nv_1 \\ y &= Cz + Du + v_2 \end{aligned} \quad (2.20)$$

Here,  $v_1$  and  $v_2$  are white noise with intensities  $R_1$  and  $R_2$ . The cross-covariance between  $v_1$  and  $v_2$  is equal to  $R_{12}$ . The observer that minimizes the estimation error  $\tilde{z} = z - \hat{z}$  is then given by (2.21).

$$\dot{\hat{z}} = A\hat{z} + Bu + K(y - C\hat{z} - Du) \quad (2.21)$$

where  $K$  is given by

$$K = (SC^T + NR_{12})R_2^{-1} \quad (2.22)$$

where  $S$  is the positive semi-definite solution to Equation 2.23

$$AS + SA^T - (SC^T + NR_{12})R_2^{-1}(SC^T + NR_{12})^T + NR_1N^T = 0. \quad (2.23)$$

## 2.5 Jacobian Linearization, equilibrium points

A time-invariant nonlinear system with no static input-output relationship can be written on the form (2.24) below. Here,  $x$  denotes the states,  $u$  the control signal and  $y$  the measurements of the states.

$$\begin{aligned} \dot{x} &= f(x(t), u(t)) = A(x) + B(x, u) \\ y &= h(x) \end{aligned} \quad (2.24)$$

Here  $f$  are  $m$  functions with  $n$  variables  $x$ . When using linear control theory (2.24) must be linearized around a stationary point, where  $f(\bar{x}, \bar{u}) = 0$ . This can be done if  $f$  is continuously differentiable in a region around  $(\bar{x}, \bar{u})$ . A first order Taylor expansion of (2.24) will then result in Equation 2.25.

$$\begin{aligned} \dot{\tilde{x}} &= \bar{A}(x - \bar{x}) + \bar{B}(u - \bar{u}) \\ \tilde{y} &= h(\bar{x}) + \bar{C}(x - \bar{x}) \end{aligned} \quad (2.25)$$

Where

$$\bar{A} = \left. \frac{dA(x)}{dx} \right|_{(\bar{x})} + \left. \frac{dB(x, u)}{dx} \right|_{(\bar{x}, \bar{u})} \quad (2.26a)$$

$$\bar{B} = \left. \frac{dB(x, u)}{du} \right|_{(\bar{x}, \bar{u})} \quad (2.26b)$$

$$\bar{C} = \left. \frac{dh(x)}{dx} \right|_{(\bar{x})} \quad (2.26c)$$

The linearized model, with  $\tilde{x} = x - \bar{x}$ ,  $\tilde{y} = y - h(\bar{x})$  and  $\tilde{u} = u - \bar{u}$  is:

$$\begin{aligned} \dot{\tilde{x}} &= \bar{A}\tilde{x} + \bar{B}\tilde{u} \\ \tilde{y} &= \bar{C}\tilde{x} \end{aligned} \quad (2.27)$$

## 2.6 Constrained motion

Constrained motion can be described as a mechanism assembled by links with certain restrictions of free movement with each link. Any relative motion arising is therefore known as constrained motion. The constrained motion can be divided into two different groups of constraints, *nonholonomic constraints* and *holonomic constraints*. Nonholonomic systems are mechanical systems with con-

straints on their velocity that are non-derivable or non-integrable from position constraints. Nonholonomic systems are typically used for robotic systems, like wheeled mobile platforms.

A set of  $k < n$  constraints is called holonomic if

$$f_i(\rho_1, \rho_2, \rho_3, \dots, \rho_n) = 0, \quad i = 1, \dots, k \quad (2.28)$$

where  $[\rho_1, \rho_2, \rho_3, \dots, \rho_n]$  are the  $n$  coordinates that describes the system. Each  $f_i$  is a smooth mapping from  $P$  to  $\mathbb{R}$ . *Smooth functions*,  $C^\infty$ , are functions  $F : \mathbb{R}^m \rightarrow \mathbb{R}^n$  where partial derivatives to all orders exists and are continuous.

Constraints of the form in (2.29) below

$$\langle w_i, \dot{\rho} \rangle = 0, \quad i = 1, \dots, k \quad (2.29)$$

are holonomic if there exists smooth functions  $f_1, \dots, f_k$  so that

$$w_i(\rho) = df_i(\rho), \quad i = 1, \dots, k \quad (2.30)$$

and nonholonomic otherwise. Equation 2.29 are called *Pfaffian* constraints.

A simple example of a nonholonomic systems are systems with rolling without slipping constraints. A way to describe nonholonomic systems is that it is a system whose states depends on what path that is taken and not only the start and end position, [7].

# 3

---

## Robot description

This chapter contains a description of the autonomous lawn mower, model Husqvarna Automower 330X, used in this master thesis.

### 3.0.1 Hardware description

The automower 330x is a four wheeled robot weighing 13.2 [kg], with the dimensions 72 [cm] long and 31 [cm] wide. The maximum angular velocity is set to 1 [rad/s]. An illustration of the automower 330x is presented in Figure 3.1.



*Figure 3.1: Illustrates the Husqvarna automower 330x.*

The automower model Husqvarna 330x is back wheel driven. The steering mechanism is done by providing different velocities on the left and the right wheel. The control signal calculated in this thesis is the angular velocity. The translation estimation, from an angular velocity to a control signal in the voltage input to left- and right engine, is done by a module that is already implemented by Husqvarna.

### **3.0.2 Measurement system**

The magnetic field strength is measured using a magnetometer sensor. The sensor is located in the mid-front of the chassi of the lawn mower. The position is approximately 10 [cm] up from the ground. In this thesis the distance to the magnetic field will be the distance along the ground from the magnetic field sensor to the magnetic loop. The zero distance is in other words when the magnetic field sensor is placed right above the magnetic loop.



# 4

---

## Modeling

This chapter contains a description of the system model of the lawn mower, feedback linearization and linearization at an equilibrium point. A stability and observability analysis will also be presented in this chapter.

### 4.1 System model

The model of the ALM can be described using a nonholonomic model due to a rolling without slipping approximation. The model of a unicycle is used to describe the system since the ALM only consists of one rigid body.

The configuration of the system can be described by a vector containing three generalized coordinates: the position coordinates,  $[x, y]$ , which is the position of the center of the ALM to the ground in a fixed frame  $(G)$ , and the angle  $\theta_m$ . The angle  $\theta_m$  is the angle of the wheel orientation with respect to the  $x$  axis.

The generalized system of a unicycle must satisfy the following constraint:

$$\dot{x} \sin \theta_m - \dot{y} \cos \theta_m = 0 \quad (4.1)$$

This constraint entails zero lateral velocity. This constraint is a typical example of a Pfaffian constraint described in section 2.6.

The model of the system is presented below:

$$u_1 = \frac{1}{2} \cdot (v_r + v_l) \quad (4.2)$$

$$u_2 = \frac{1}{2} \cdot (v_r - v_l) \quad (4.3)$$

$$\dot{x} = v \cdot \cos(\theta_m) \quad (4.4a)$$

$$\dot{y} = v \cdot \sin(\theta_m) \quad (4.4b)$$

$$\dot{\theta}_m = u_2 \quad (4.4c)$$

$$v = u_1 \quad (4.4d)$$

where  $v_r$  and  $v_l$  are the right- and left wheel velocity, respectively  $y$  and  $x$  are the current position in the global coordinate system ( $G$ ), and  $\theta_m$  is the vehicle's orientation with respect to the fixed reference frame.

In order to simplify the system a transformation between the global coordinate system ( $G$ ) to a local coordinate system ( $L$ ) is performed. The global coordinate system is a fixed system whilst the local system is defined on a curvature. An illustration of the global and the local coordinate systems is shown in Figure 4.1 below, [8][3].

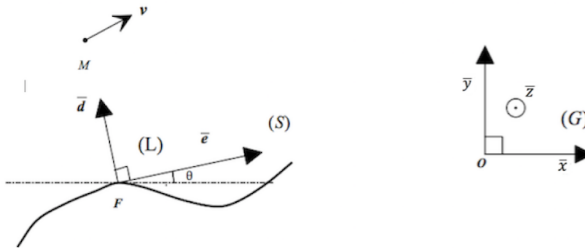


**Figure 4.1:** Illustrates the local coordinate system ( $L$ ) and the global coordinate system ( $G$ ). The point  $F$  is the orthogonal projection of the point  $M$  on to the curve.  $\theta$  is the angle between the tangential vector of the curve in point  $F$  and the local coordinate system vector  $\bar{e}$ . The curve is denoted ( $S$ ).

The point  $F$  is the orthogonal projection of the point  $M$  onto the curve, [12]. The coordinates of point  $M$  are  $(0, z, 0)$  in the local frame  $(L) = (F; \bar{e}, \bar{d}, \bar{z})$  and  $(x, y, 0)$  in the fixed reference frame  $(G) = (O; \bar{x}, \bar{y}, \bar{z})$ . The position of  $M$  in the ( $G$ )-plane is characterized by the cartesian coordinates  $(x, y)$ , and in the ( $L$ )-plane the variables  $(l, z)$ .

A classical mechanics law will then give the translation between these two coordinate systems:

$$\left(\frac{d\overline{OM}}{dt}\right)_G = \left(\frac{d\overline{OF}}{dt}\right)_G + \left(\frac{d\overline{FM}}{dt}\right)_L + \omega_0 \times \overline{FM} \quad (4.5)$$

where

$$[\overline{FM}]_L = \begin{pmatrix} 0 \\ z \\ 0 \end{pmatrix} \quad \text{and} \quad [\overline{\omega}_0]_G = \begin{pmatrix} 0 \\ 0 \\ \dot{\theta} = s_0(l)\dot{l} \end{pmatrix} \quad (4.6)$$

The vector  $[\overline{\omega}_0]$  is the rotational velocity of the local frame ( $L$ ) with respect to ( $G$ ). The symbol  $\left(\frac{d}{dt}\right)_L$  is derivation with respect to the frame ( $L$ ). Lastly,  $s_0(l)$  is the curvature of the path in ( $L$ ).

The rotation matrix from ( $G$ ) to ( $L$ ),  $R_r$ , is defined below:

$$R_r = \begin{pmatrix} \cos \theta & \sin \theta & 0 \\ -\sin \theta & \cos \theta & 0 \\ 0 & 0 & 1 \end{pmatrix} \quad (4.7)$$

Equation 4.5 then results in:

$$\begin{pmatrix} \dot{l} \\ \dot{z} \\ 0 \end{pmatrix} = R_r \begin{pmatrix} \dot{x} \\ \dot{y} \\ 0 \end{pmatrix} + \begin{pmatrix} s_0(l)z\dot{l} \\ 0 \\ 0 \end{pmatrix} \quad (4.8)$$

This will then give the following equations:

$$\dot{l} = \frac{1}{(1 - s_0(l)z)} (\cos \theta \quad \sin \theta) \cdot \begin{pmatrix} \dot{x} \\ \dot{y} \end{pmatrix} \quad (4.9a)$$

$$\dot{z} = (-\sin \theta \quad \cos \theta) \cdot \begin{pmatrix} \dot{x} \\ \dot{y} \end{pmatrix} \quad (4.9b)$$

Using Equation 4.4 in Equation 4.9 will give:

$$\begin{aligned} \dot{l} &= \frac{1}{(1 - s_0(l)z)} v \cdot \cos \tilde{\theta} \\ \dot{z} &= v \cdot \sin \tilde{\theta} \\ \dot{\tilde{\theta}} &= \dot{\theta}_m - \dot{\theta} = u_2 - u_{2,0} \end{aligned} \quad (4.10)$$

where  $v$  is set to be a constant velocity in this thesis and  $u_2$  comes from Equation 4.3. The scalar  $u_{2,0}$  represents the direction of the magnetic loop. The basic problem in this thesis concerns a none curved magnetic loop. This means that  $u_{2,0}$  and  $s_0$  will be approximated to zero.

## 4.2 Feedback linearization

To compensate for the nonlinearities in the model described above, a form of feedback to reduce the nonlinear characteristics is a common choice of action. When the nonlinearities are reduced one can control the system as if it were linear. In some cases, the feedback can be done to the extent that the system is exactly linearized.

In this section feedback linearization will be implemented on the system described in 4.10. The state  $l$  will not be of interest for this thesis, since  $l$  does not affect the controller performance. Therefore it will be disregarded in the feedback linearization. If  $s_0 = 0$ ,  $u_{2,0} = 0$ ,  $u_2 = u$  and  $v = a$  (where  $a$  is a constant), the system can be described according to Equation 4.11.

$$\begin{aligned}\dot{z} &= a \cdot \sin \tilde{\theta} \\ \dot{\tilde{\theta}} &= u\end{aligned}\tag{4.11}$$

If  $y$  is chosen as  $y = z$ , it holds that  $\dot{y} = a \cdot \sin \tilde{\theta}$  and  $\ddot{y} = a \cdot \cos \tilde{\theta} \cdot \dot{\tilde{\theta}} = a \cdot \cos \tilde{\theta} \cdot u$ . This results in the relative degree of the system as  $v = 2$ . New variables are introduced and presented in Equation 4.12.

$$\begin{aligned}\epsilon_1 &= z \\ \epsilon_2 &= a \cdot \sin \tilde{\theta}\end{aligned}\tag{4.12}$$

The derivatives are presented in (4.13).

$$\begin{aligned}\dot{\epsilon}_1 &= \dot{z} = a \cdot \sin \tilde{\theta} = \epsilon_2 \\ \dot{\epsilon}_2 &= a \cdot \cos \left( \arcsin \left( \frac{\epsilon_2}{a} \right) \right) \cdot u\end{aligned}\tag{4.13}$$

If the feedback is chosen according to Equation 4.14 the nonlinear characteristics will cancel out.

$$u = \frac{\ddot{y}}{a \cdot \cos \left( \arcsin \left( \frac{\epsilon_2}{a} \right) \right)}\tag{4.14}$$

In Equation 4.14,  $\arcsin \left( \frac{\epsilon_2}{a} \right) = \tilde{\theta}$  and  $|\tilde{\theta}| < \frac{\pi}{2}$ . The system is now input-output linearized and linear control theory can be applied.

The state space model for the new, linearized system is presented in Equation 4.15.

$$\begin{aligned}\dot{\epsilon} &= \tilde{A}\epsilon + \tilde{B}u = \begin{pmatrix} 0 & 1 \\ 0 & 0 \end{pmatrix}\epsilon + \begin{pmatrix} 0 \\ 1 \end{pmatrix}u \\ y &= \tilde{C}x = \begin{pmatrix} 1 & 0 \end{pmatrix}x\end{aligned}\quad (4.15)$$

An analysis whether the states in Equation 4.15 are observable or not is done using the observability matrix,  $\mathcal{O}$ , see (4.16).

$$\mathcal{O} = \begin{pmatrix} \tilde{C} \\ \tilde{C}\tilde{A} \end{pmatrix} = \begin{pmatrix} 1 & 0 \\ 0 & 1 \end{pmatrix}\quad (4.16)$$

Since  $\det(\mathcal{O}) \neq 0$  the system is observable. The poles of an observer can thus be placed arbitrarily. Further more, to see if the system is controllable the controllability matrix,  $\mathcal{S}$  is investigated and presented below in Equation 4.17.

$$\mathcal{S} = \begin{pmatrix} \tilde{B} & \tilde{A}\tilde{B} \end{pmatrix} = \begin{pmatrix} 0 & 1 \\ 1 & 0 \end{pmatrix}\quad (4.17)$$

Since  $\det(\mathcal{S}) \neq 0$  the system is controllable.

### 4.2.1 Lyapunov analysis

Lyapunov's stability test is a commonly used method when studying the stability characteristics of a dynamic system. If there exists a function  $V$  that satisfies the conditions presented in Equations 2.10-2.12, the equilibrium point is globally asymptotically stable. The equilibrium point investigated is  $[z, \tilde{\theta}, u] = [0, 0, 0]$ .

For the system presented in Equation 4.11, it can be shown that if  $V$  is chosen as

$$V = \frac{1}{2}(k_1 z^2 + \tilde{\theta}^2), \quad k_1 > 0\quad (4.18)$$

with  $u$  chosen so that  $\dot{V} < 0$  for all  $z$  and  $\tilde{\theta} \neq 0$ .

$$\begin{aligned}\dot{V} &= k_1 \cdot z \cdot \dot{z} + \tilde{\theta} \cdot \dot{\tilde{\theta}} = k_1 \cdot z \cdot v \cdot \sin \tilde{\theta} + \tilde{\theta} \cdot u = \\ &= \int u = -k_2 \cdot \tilde{\theta} - k_1 \cdot v \cdot \frac{\sin \tilde{\theta}}{\tilde{\theta}} \cdot z \int = \\ &= -k_2 \tilde{\theta}^2 < 0 \quad \forall z, \tilde{\theta} \neq 0, k_2 > 0.\end{aligned}\quad (4.19)$$

Equation 4.19 satisfies all conditions for the Lyapunov stability test.

### 4.3 Linearization in the equilibrium point

The nonlinear system presented in Equation 4.10 can be written in the form shown in Equation 2.27. The state  $l$  will not be considered since it does not affect the outcome of the controller. Therefore, it is not a state of interest. With the use of the Jacobian linearization of the nonlinear model, the model is linearized at the point  $[z, \tilde{\theta}, u] = [0, 0, 0]$ .

From Equation 2.26 the following expression is received:

$$\begin{aligned}\bar{A} &= \left. \frac{dA(x)}{dx} \right|_{(0)} + \left. \frac{dB(x, u)}{dx} \right|_{(0,0)} = \left. \begin{pmatrix} 0 & v \cos \tilde{\theta} \\ 0 & 0 \end{pmatrix} \right|_{(0,0)} = \begin{pmatrix} 0 & v \\ 0 & 0 \end{pmatrix} \\ \bar{B} &= \left. \frac{dB(x, u)}{du} \right|_{(0,0)} = \begin{pmatrix} 0 \\ 1 \end{pmatrix} \bigg|_{(0,0)} = \begin{pmatrix} 0 \\ 1 \end{pmatrix} \\ \bar{C} &= \left. \frac{dh(x)}{dx} \right|_{(0)} = (1 \quad 0)\end{aligned}\tag{4.20}$$

The resulting model is presented below in Equation 4.21:

$$\begin{aligned}\begin{pmatrix} \dot{z} \\ \dot{\tilde{\theta}} \end{pmatrix} &= \begin{pmatrix} 0 & v \\ 0 & 0 \end{pmatrix} \begin{pmatrix} z \\ \tilde{\theta} \end{pmatrix} + \begin{pmatrix} 0 \\ 1 \end{pmatrix} u \\ y &= (1 \quad 0) \begin{pmatrix} z \\ \tilde{\theta} \end{pmatrix}\end{aligned}\tag{4.21}$$

### 4.4 Discretization of the time-continuous model

The theory that has been presented this far holds for time continuous systems. In reality, the signals have been sampled. The controllers and observers used in this thesis are implemented in a time discrete sense.

Discretizing the systems provided in Equations 2.27 and 4.21 with zero-order-hold will have the same structure as Equation 4.22.

$$\begin{aligned}x(kT + T) &= Fx(kT) + Gu(kT) \\ y(kT) &= Hx(kT)\end{aligned}\tag{4.22}$$

where

$$F = e^{\bar{A}T}, \quad G = \int_0^T e^{\bar{A}t} \bar{B} dt, \quad H = \bar{C}\tag{4.23}$$

The result of the discretized model is presented in Equation 4.24 below

$$\begin{aligned}x(kT + T) &= \begin{bmatrix} 1 & vT \\ 0 & 1 \end{bmatrix} x(kT) + \begin{bmatrix} vT^2/2 \\ T \end{bmatrix} u(kT) \\ y(kT) &= \begin{bmatrix} 1 & 0 \end{bmatrix} x(kT)\end{aligned}\tag{4.24}$$

Here,  $T$  is the sample time and  $v$  is the constant average, velocity of the ALM.





# 5

---

## Magnetic field navigation

### 5.1 Biot - Savart Law

The lawn mower navigates using one magnetic field sensor and magnetic loops buried in the lawn. Using Biot-Savarts law the distance between the vehicle to the magnetic loop can be estimated. Biot-savart is a physical law that describes the size of the magnetic flux density  $B$ , caused by an electric current  $I$ . In Equation 5.1, the Biot-Savarts law is provided, [2].

$$\bar{\mathbf{B}} = \oint_{C'} d\mathbf{B} \quad (5.1)$$

where  $d\mathbf{B}$  is given by:

$$d\mathbf{B} = \frac{\mu_0 I}{4\pi} \left( \frac{dl' \times \mathbf{a}_R}{R^2} \right) \quad (5.2)$$

where  $\mathbf{a}_R$  is the unit vector from the source point to the field point. Vector  $\mathbf{R}$  is the distance between  $dl'$  at  $(x', y', z')$  to the field point  $(x, y, z)$  and  $C'$  is the path of the current.

## 5.2 Distance from the magnetic loop to vehicle

To be able to estimate the distance between the magnetic loop and the magnetic field sensor on the vehicle, some assumptions were made in order to simplify the calculations. A current  $I$  flows through a straight magnetic loop and the magnetic loop is assumed to have an endless length. The distance vector from the source element  $dz'$  to the point  $P$  is shown in Equation 5.3 and in Figure 5.1.

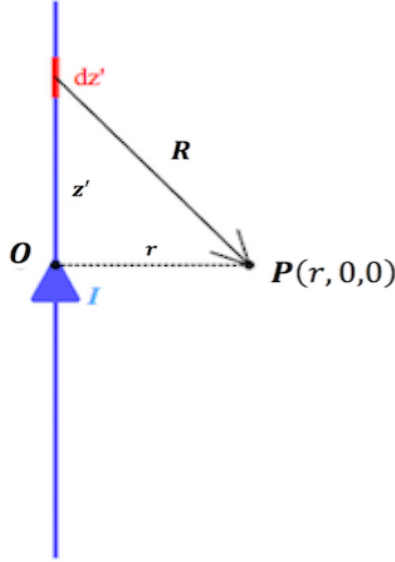


**Figure 5.1:** Illustrates the current  $I$  running through a straight wire and position  $P$  coordinates relative to the wire. The differential  $dz'$  is a source element.

$$\mathbf{R} = \mathbf{a}_r r - \mathbf{a}_z z' \quad (5.3)$$

where  $z'$  is illustrated in Figure 5.1, and where

$$dz' \times \mathbf{R} = \mathbf{a}_z dz' \times (\mathbf{a}_r r - \mathbf{a}_z z') = a_\phi r dz' \quad (5.4)$$

$$\bar{\mathbf{B}} = \frac{\mu_0 I}{4\pi} \int_{-\infty}^{\infty} \frac{dz' \times \mathbf{R}}{R^3} = \mathbf{a}_\phi \frac{\mu_0 I}{4\pi} \int_{-\infty}^{\infty} \frac{r dz'}{(z'^2 + r^2)^{3/2}} = \frac{\mathbf{a}_\phi \mu_0 I}{2\pi r} \quad (5.5)$$

where  $\mathbf{a}_\phi$  is a unit vector in  $\phi$  direction in cylindrical coordinates. From Equation 5.5 the distance,  $r$ , can be estimated given  $\bar{\mathbf{B}}$  and  $I$ .

## 5.3 Measured magnetic field

In reality, the theory mentioned above only applies for special conditions, such as that the magnetic loop is straight and that it is infinite. In order to navigate using the magnetic field, the magnetic field was measured and mapped to a distance. Figure 5.2 illustrates the magnetic field strength mapped against the distance to the magnetic loop.

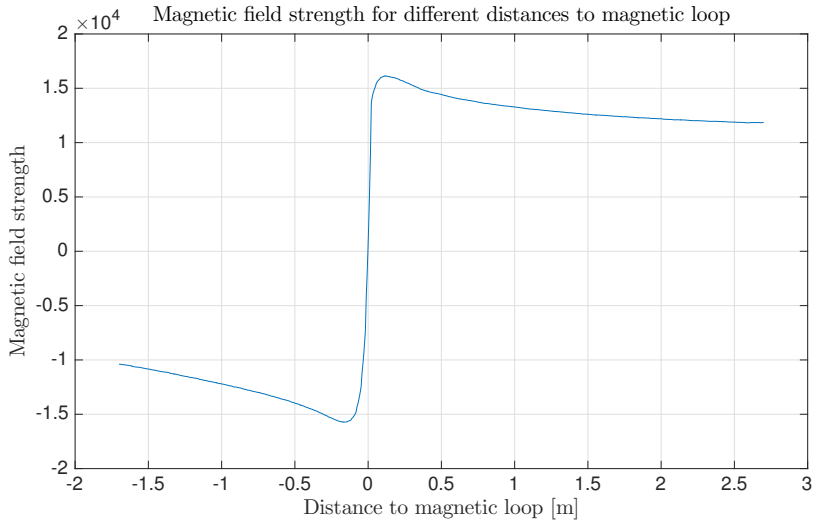


**Figure 5.2:** The magnetic field strength mapped against the distance to the magnetic loop.

As shown in Figure 5.2, some magnetic field values correspond to two different distances to the magnetic field. These physical properties of the magnetic field along with big standard deviations in the measurements makes it a problematic issue.

Table 5.1, presented below, is a table of the standard deviation of the measured field strength. These measurements were made when the vehicle was stationary at different distances to the magnetic loop.

From the standard deviation it can be noticed that the closer to the magnetic loop the measurements are, the more noisy the measurements of the magnetic field strength are. This will in turn also make the interpretation of the magnetic field strength even more difficult.

**Table 5.1:** Standard deviation of the magnetic field strength for different measured distances.

Distance, [m]	Standard deviation, $\sigma$
0.0	863.7
0.1	6.9
0.2	7.3
0.3	6.0
0.5	5.2

### 5.3.1 Distance to the magnetic loop using *trend-equations*

When estimating the distance to the magnetic loop, there are many different difficulties to take into consideration. There are often two different distances that correspond to one magnetic field value and there are a steep change near the zero distance. In order to be able to map the distance to the magnetic value, an approximative approach is used, where a trend function is estimated. The estimated trend function uses the measured magnetic field strength previously demonstrated in Figure 5.2. The trend function is displayed in Equation 5.6.

$$r(x) = \text{sgn}(x) \cdot 4817.6 \cdot e^{(-6 \cdot 10^{-4} \cdot |x|)} \quad (5.6)$$

where  $|x|$  is the measured magnetic field strength from the magnetic loop and  $\text{sgn}(x)$  is the sign function. The steep part around zero is cut out when estimating the function of the distance, since the steep part cannot be explained by a trend function. Therefore the function is only valid for distances,  $r$ , larger than the distance corresponding to the steep part of the magnetic field, see Figure 5.2. If  $x$  is negative the ALM is navigating outside of the magnetic loop.

The following algorithm, Algorithm 1, contains a description of how to estimate the distance. Line 7 displays the conditions of when the change in the distance is too big. When close to the magnetic loop, the trend Equation 5.6 will estimate a big leap in the distance to the magnetic loop from one sample to the next. Instead of saving this value, a comparison between the old value and the newly sampled value is performed. If the difference is greater than 0.2 [m] (which is a distance that the ALM is not capable to move in one sample) the newly measured value will be rejected and instead the value from the previous sample will be used as the measured distance.

**Algorithm 1** Distance to magnetic loop, trend-equations

---

```

1: procedure DISTANCEFROMMAGLOOP(magField, rOld) ▷
2:   if magField ≥ 0 then ▷ if inside the magnetic loop
3:      $r = 4817,6 \cdot e^{(-6 \cdot 10^{-4} \cdot |magField|)}$ 
4:   else
5:      $r = -4817,6 \cdot e^{(-6 \cdot 10^{-4} \cdot |magField|)}$ 
6:   end if
7:   if  $||rOld| - |r|| \geq 0.2$  then ▷ If the change in distance is to big
8:      $r = rOld$  ▷ then the magnetic loop is close
9:   end if
10:  rOld=r
11:  return r ▷
12: end procedure

```

---

**5.3.2 Distance to the magnetic loop using *look-up table***

Another approach to address the difficulties in estimating the distance to the magnetic loop is by using a look-up table. The magnetic field of the magnetic loop is then mapped against a distance to the magnetic loop. In this way, if one magnetic field strength corresponds to two different distances, the challenge will instead be to choose the correct distance out of these two possibilities.

The following algorithms, Algorithm 2 and 3, contains the description of how to estimate the distance to the magnetic loop by the use of a look-up table. The case where two different distances are mapped against one magnetic field value is treated from row 3 to 18. The algorithms use the shape of the derivative of the magnetic field. The derivative will be big close to the magnetic loop and small when further away from the loop.

Algorithm 2 estimates the derivative by estimating the difference of the last sampled magnetic field value to the newly sampled value.

Another approach to select the right distance when two values are found in the look-up table, is to use an average of earlier saved sampled values. This method is presented in Algorithm 3.

How many values that should be taken into consideration when estimating the average is a design parameter and will be discussed further in section 6.3.1. Algorithm 3 uses three saved values.

---

**Algorithm 2** Distance to magnetic loop, look-up table
 

---

```

1: procedure DISTANCEFROMMAGLOOP(magField, oldMagField, z)           ▶
2:   find the distances corresponding to the magField and save them as
   value1 and value2.
3:   if two distances are found then
4:     if  $|OldMagField - magField| \geq 500$  then ▶ Close to the magnetic loop
5:       if  $|value1| \geq |value2|$  then
6:          $r = value2$ 
7:       else
8:          $r = value1$ 
9:       end if
10:    else
11:      if  $|value1| \geq |value2|$  then           ▶ Far away from the magnetic loop
12:         $r = value1$ 
13:      else
14:         $r = value2$ 
15:      end if
16:    end if
17:  else
18:     $r = value1$            ▶ Only one mapped distance to that magField
19:  end if
20:   $OldMagField = magField$ 
21:  return  $r$ 
22: end procedure

```

---

---

**Algorithm 3** Distance to magnetic loop, look-up table
 

---

```

1: procedure DISTANCEFROMMAGLOOP(magField, magField0, magField1,
   magField2, z) ▷
2:   find the distances corresponding to the magField and save them as
   value1 and value2.
3:   if two distances are found then
4:     average1 = (magField + magField0 + magField1)/3
5:     average2 = (magField0 + magField1 + magField2)/3
6:     if |average1 – average2| ≥ 300 then ▷ Close to the magnetic loop
7:       if |value1| ≥ |value2| then
8:         r = value2
9:       else
10:        r = value1
11:      end if
12:    else
13:      if |value1| ≥ |value2| then ▷ Far away from the magnetic loop
14:        r = value1
15:      else
16:        r = value2
17:      end if
18:    end if
19:  else
20:    r = value1 ▷ Only one mapped distance to that magField
21:  end if
22:  magField2 = magField1
23:  magField1 = magField0
24:  magField0 = magField
25:  return r
26: end procedure

```

---





# 6

---

## Results

In this chapter, the main results from this thesis are presented. The first section describes the results from the simulation in Simulink and the second section contains results from simulations using Gazebo. The results when testing the controllers on real hardware are presented in the third section.

As previously mentioned, all states can not be measured. In order to estimate states a Kalman filter has been implemented. Since the measurements of the distance to the magnetic loop are unreliable an observer is required. The observer should be fast enough to adjust adequately when the distance to the magnetic loop changes. For robustness against measurement errors, the speed of the observer must be chosen carefully. When designing the weight matrices of the Kalman filter, tests were performed in order to model the measurement and model errors. Unfortunately, this resulted in that the errors could not be modeled as white noise. Thus the theory for estimating the best weight matrices, by the knowledge of its behavior, could not be applied. Instead, the weight matrices were produced by testing both in simulations and on the hardware.

The calculation of the feedback gain was performed by using an linear quadratic controller. Upon implementing the observer, it is important that the observer is faster than the controller. This was accomplished by studying the eigenvalues of both the observer and the closed loop with the calculated feedback gain.

After several tests, the observer gain for this thesis was chosen as  $K = [0.8327, 0.6658]$ . This resulted in the eigenvalues  $\lambda = [0.1795, 0.9878]$ . The feedback gain was then estimated using linear quadratic control. The feedback gain used in this thesis was  $L = [2.1722, 1.1416]$ . The eigenvalues of the closed loop system were  $\lambda = [0.9711 + 0.0281i, 0.9711 - 0.0281i]$ . Since these are the eigenvalues of a time discrete system, the distance to the unit circle determines

the speed of the observer and the feedback. The closer to the unit circle, the slower characteristics can be expected. After observing the eigenvalues of both the observer and the closed loop system it can be concluded that the observer and the closed loop system does not differ greatly in terms of speed. When designing the observer one usual approach is to design the observer to be faster than the closed loop system, but since they were similar in speed the end result was still good.

## 6.1 Results from simulations i Simulink

The first step when evaluating the controllers was to implement the non-linear model along with the controllers into the simulation environment Simulink. The results, after transmitting a reference signal of the distance to the magnetic loop in to the system, was plotted in MATLAB. The weight matrices of the LQ controller and the Kalman filter were altered depending on how the results appeared in the plots.

Figure 6.1 illustrates a step response of the system using feedback linearization and Figure 6.2 illustrates the results of a step response using linearization at an equilibrium point and LQ-control. The step, in both of these figures, were taken from 0 [m] to 0.5 [m]. The Kalman gain in these figures was  $K = [0.8327, 0.6658]$  and the feedback gain was  $L = [2.1722, 1.1416]$ .

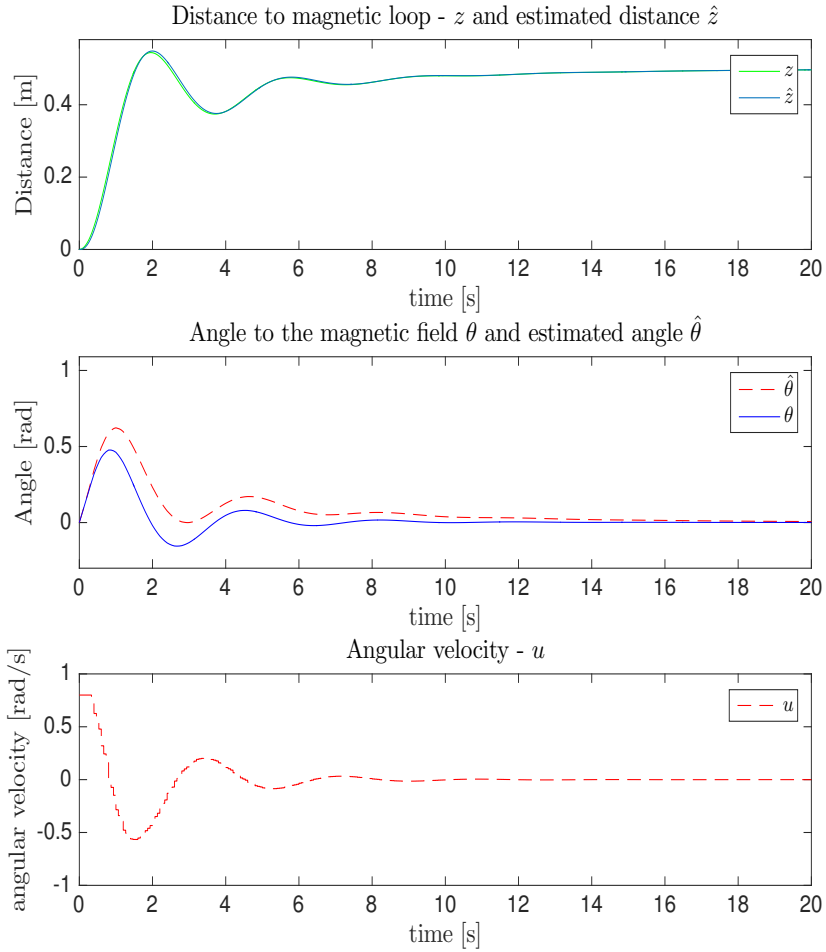


**Figure 6.1:** Illustrates a step response in the simulation environment Simulink, using feedback linearization. The feedback gain is set to  $L = [2.1721, 1.1449]$  and the observer gain is set to  $K = [0.8327, 0.6658]$ . The first graph illustrates the distance to the magnetic loop, where the blue line represents the observed state and the green illustrates the measured distance. The second graph illustrates the angle towards the magnetic loop. The red line is the observed angle and the blue line is the measured angle. The third graph illustrates the control signal, angular velocity.

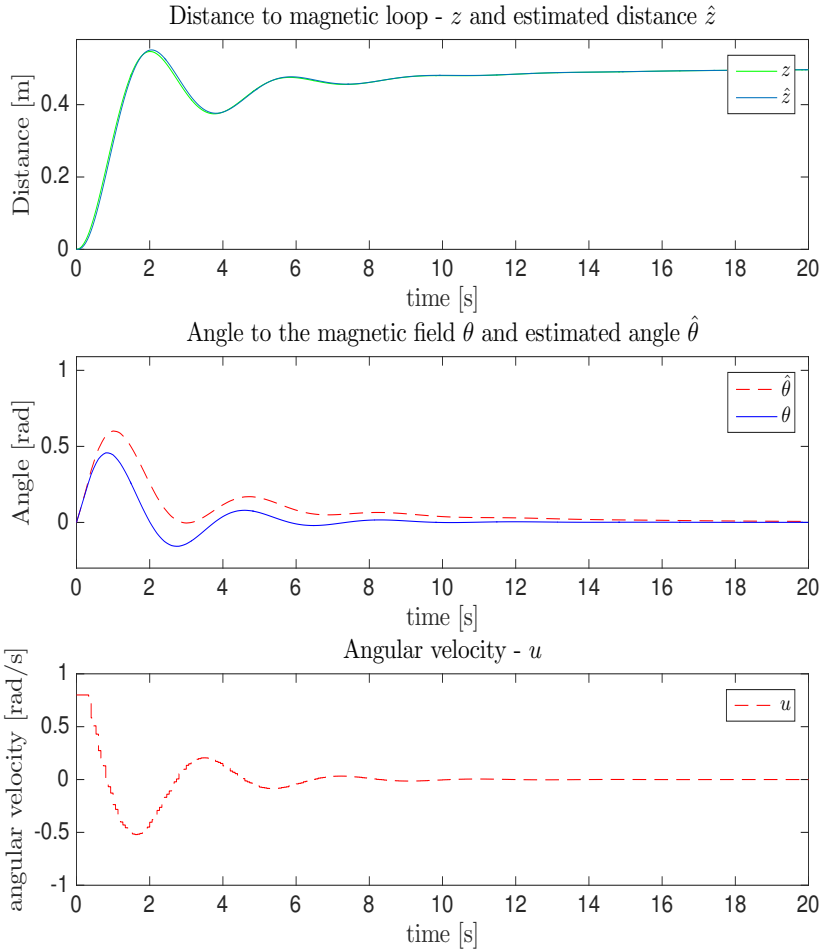


**Figure 6.2:** Illustrates a step response in the simulation environment Simulink using an LQ-controller and linearization in equilibrium point. The feedback gain is set to  $L = [2.1721, 1.1449]$  and the observer gain is set to  $K = [0.8327, 0.6658]$ . The first graph illustrates the distance to the magnetic loop, where the blue line represents the observed state and the green illustrates the measured distance. The second graph illustrates the angle towards the magnetic loop. The red line is the observed angle and the blue line is the measured angle. The third graph illustrates the control signal, angular velocity.

The step is taken in the distance,  $z$ , from 0 to 0.5 [m]. That is, the relative distance from the magnetic loop. The step response in the two Figures, 6.2 and 6.1, look very similar. They both use the same feedback gain and observer gain. The only difference is how the control signal is calculated. Figure 6.2 uses an LQ-controller where  $u$  is estimated using the expression in Equation 2.16. Figure 6.1 uses feedback linearization and the control signal is calculated using Equation 4.14 where  $\bar{u}$  is calculated according to Equation 2.16.

## 6.2 Results from Gazebo simulations

After evaluating the various controllers and observers in Simulink, they were implemented and tested in the ROS enabled simulation environment Gazebo. Figure 6.3 illustrates a simulation of the lawn mower around a simulated lawn in Gazebo, with a mapped magnetic field. The magnetic field strength is mapped in each position of the virtual lawn. The simulated magnetic field in the Gazebo environment is not an exact model of the magnetic field in reality. In order to use the simulation environment in Gazebo the magnetic field in the simulation environment was measured and by using a trend-function, see Algorithm 1 (with another  $r(x)$ ), a simulation was made.

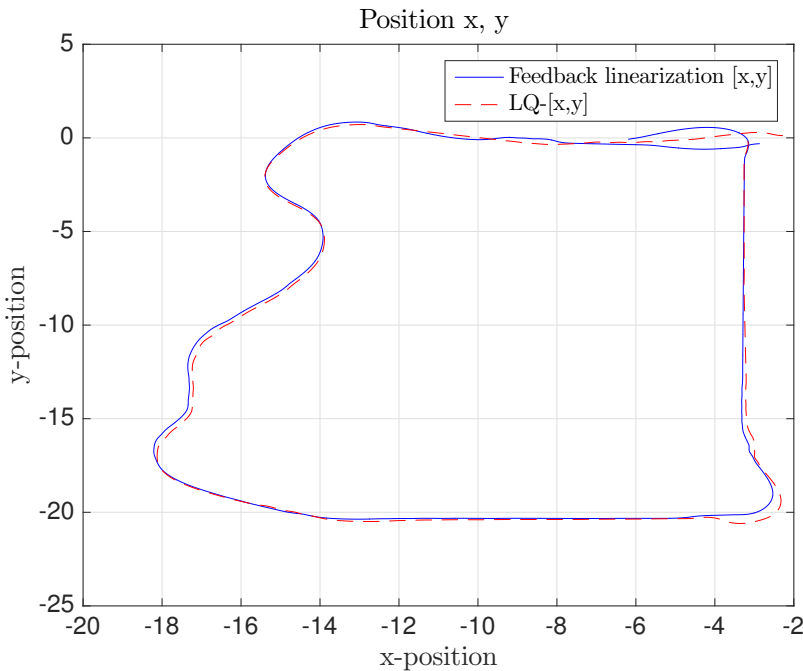


**Figure 6.3:** Illustrates a simulation in the simulation environment Gazebo. The blue line illustrates the path taken when feedback linearization was used and the red line when the LQ-controller along with linearization in an equilibrium point was used.

Figure 6.3 illustrates one lap around the lawn in the Gazebo simulation environment. Even though the true position of the magnetic loop is not illustrated in the Figure 6.3 above, the main behavior of the two different controllers can be studied. One thing that is clear is that the controllers are similar. The only thing that stands out is the ability to navigate in corners. The controller based on feedback linearization appears to have a smaller overshoot in tight corners. This is clearly visible in the right bottom corner in Figure 6.3.

## 6.3 Hardware - Husqvarna Automower 330X

When the controllers were evaluated outdoors, other factors not shown in the simulation environment appeared. The fact that the lawn was not always flat and contained tufts of grass affected the behavior of the ALM. Shown in Table 5.1, the deviation of the magnetic field strength varied depending on the distance to the magnetic loop. The magnetic field strength sensor was also sensitive towards the contribution of a magnetic loop close by. This complicated the navigation, particularly in and around corners. The contribution in the corners could have been likened as two magnetic loops close to each other. This then affected the distance estimation and navigation of the ALM.

The following tests, unless otherwise noted, brought up and discussed in this section are performed on a track with many turns and with only short sections of non-curved loop. This will affect the appearance of the graphs when the mower tries to follow the reference distance. When evaluating the controllers this was an active choice since the most challenging case to control is a curved magnetic loop.

The following tests are performed using an altered saturation of the control signal depending on the current measured control error. The hardware has an angular velocity limit of 1 [rad/s], therefore a maximum saturation was implemented with  $u \leq 0.8$  [rad/s]. The saturation interval was designed to be smaller when the distance to the control error was reduced. The interval for when the saturation level was altered depended on what reference distance the lawn mower was supposed to follow. This way, the controller was slower when closer to the reference distance. When  $\tilde{z} < 0.1$  and  $0.2 < z_{ref} < 0.3$  the saturation was set to  $u \leq \pm 0.15$  [rad/s]. When  $\tilde{z} < 0.15$  and  $z_{ref} \leq 0.2$  the saturation was set to  $u \leq \pm 0.15$  [rad/s]. The variable  $\tilde{z}$  is the control error,  $z_{ref}$  is the reference distance to the magnetic loop and  $u$  is the control signal, see Algorithm 4 in Appendix A. The reason for the altered saturation with different distances was the unreliable measurements. The standard deviation, presented in Table 5.1, increased when closer to the magnetic loop. Therefore, the saturation interval was altered depending on the reference.

### 6.3.1 Look-up table

The design parameters of the controller, the observer and the way to read the magnetic field strength makes the parameters in the system difficult to trim.

The case where the reference distance was set to be smaller than 0.2 [m] was the most challenging case for the controller. This was because of the nature of the magnetic field caused by the magnetic loop. As could be seen in Figure 5.2, the changes of the magnetic field was most difficult around the zero distance. This along with measurement noise, made the distance estimate difficult. Figure 6.4 illustrates two tests performed on the lawn with the reference signal set to 0 [m]. The difference between these tests are the different methods when making the choice of which value of the two found in the look up table that should be chosen.

In the A and B graphs the Algorithm 2 have been used. In the C and D graphs the Algorithm 3 have been used. The green line symbolizes the first found mapped distance in the look-up table, and the yellow the second found mapped distance. The dotted red line symbolizes the distance chosen according to Algorithms 2 and 3 from above. The blue line in the A and C graph is the observed state. The blue line in the B and D graph is the control signal during the test. Both of these tests used the same controller structure and observer gain. The controller used are feedback linearization with  $L = [2.1721, 1.1449]$ . The observer gain used in these tests was  $K = [0.8326, 0.6658]$ . The effect that can be seen in Figure 6.4 is that there are less spikes when estimating either `value1` or `value2` when using Algorithm 3. A spike can be interpreted as the robot moving a unreasonably long distance in one sample. Fewer spikes in the state estimation is desirable and therefore Algorithm 3 is preferred.

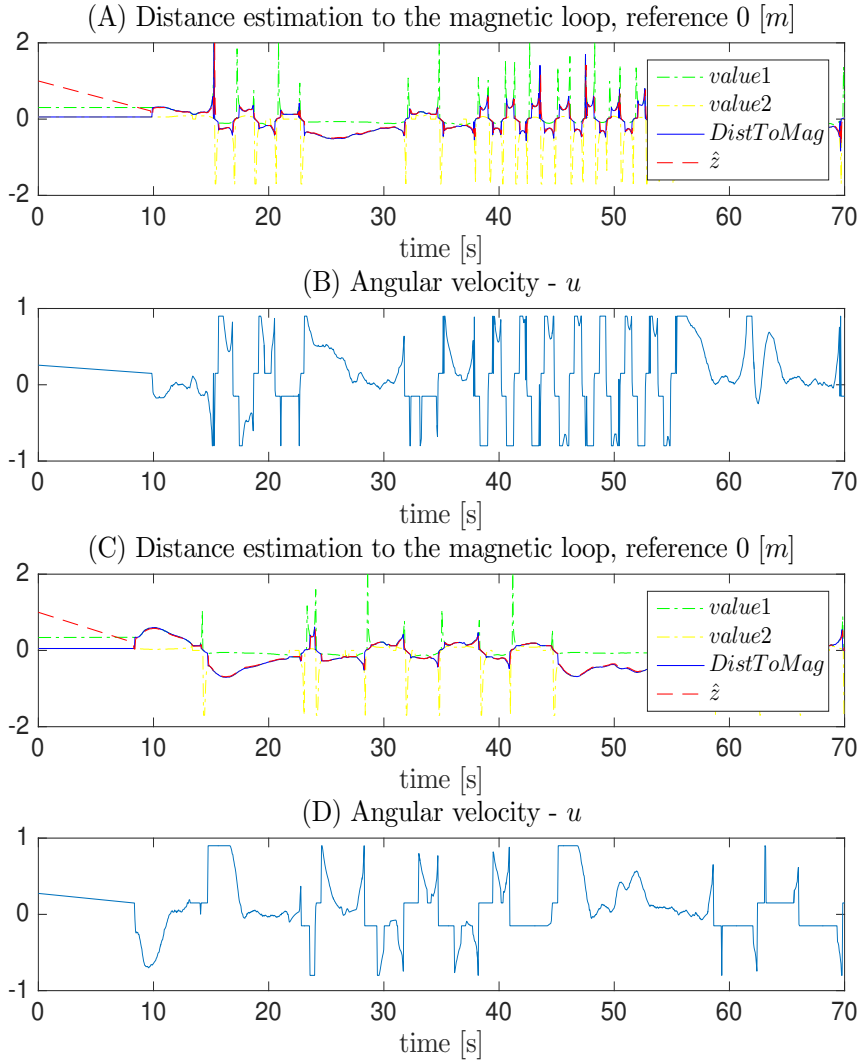
Deciding the number of saved values used in Algorithm 3 is a trade off between the ability to react to fast changes in the magnetic field and to low pass filter the measurements in order to minimize the number of spikes in the distance estimation. The number of saved values that should be used was decided through tests. The best result after these tests where three saved values, as shown in Algorithm 3. If more values were saved in the comparison the measurements would not show a large enough derivative, and the chosen magnetic field value would be recognized as the value furthest away from the magnetic loop.

Figure 6.5 illustrates two tests with two different reference distances to the magnetic loop. The tests uses the same controller, observer and algorithm as previously used in Figure 6.4 C and D. The reference in graph A and B is set to 0 [m] and in C and D to 0.3 [m].

When it comes to following the reference distance, it is clear from Figure 6.5 that it is much easier to follow the reference of a 0.3 [m] distance than straddling the loop. When the magnetic loop is non-curved, the controller error is close to zero for the test with the reference 0.3 [m] from the loop. With a reference of 0 [m] from the loop following the reference is always a struggle, even when straight.

The two controller methods presented in this thesis are very similar. To compare the two controller strategies, a step response test was performed. The step was taken from 1 [m] to 0.2 [m]. The magnetic loop was straight. The test is presented in Figure 6.6. From this figure, it can be distinguished that linearization in equilibrium point with LQ-controller is faster than feedback linearization. The overall appearance of the two controller strategies are very similar.





**Figure 6.4:** Graph A and B uses Algorithm 2 when estimating the distance to the magnetic loop. Graph C and D uses Algorithm 3.

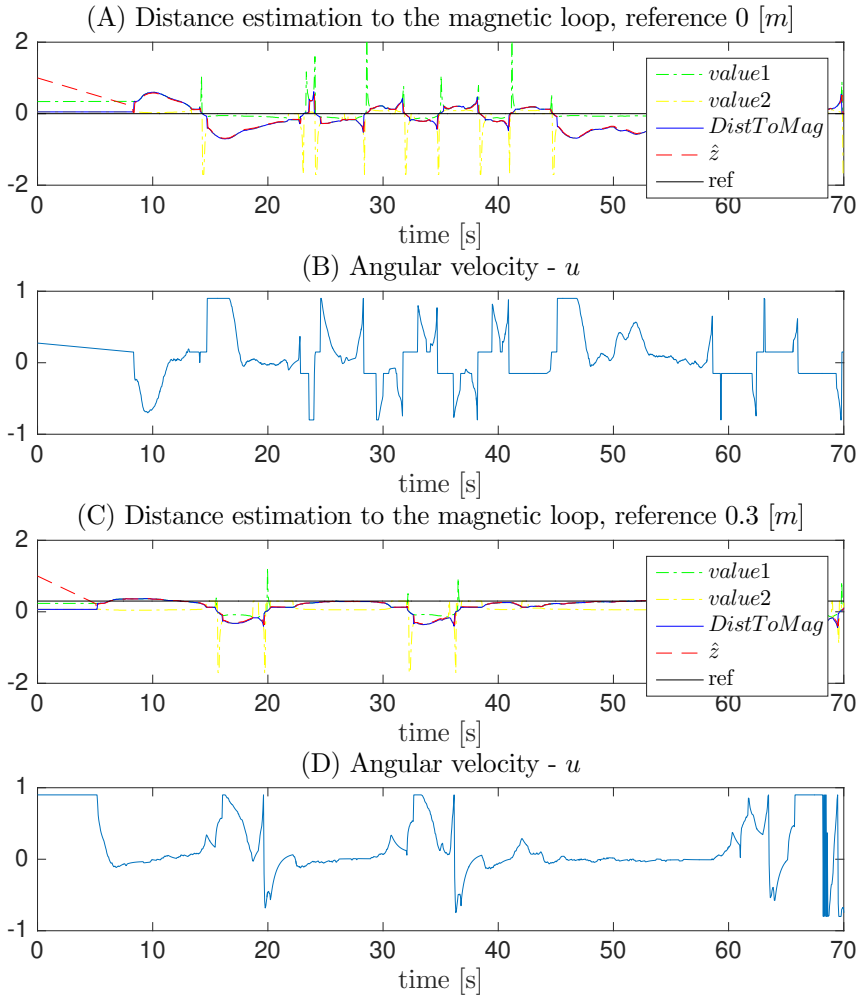


**Figure 6.5:** Two different test with the same feedback and observer gain but with different reference distances. The reference to the magnetic loop is set to 0 [m] in the A and B graphs, and 0.3 [m] in the C and D graphs.

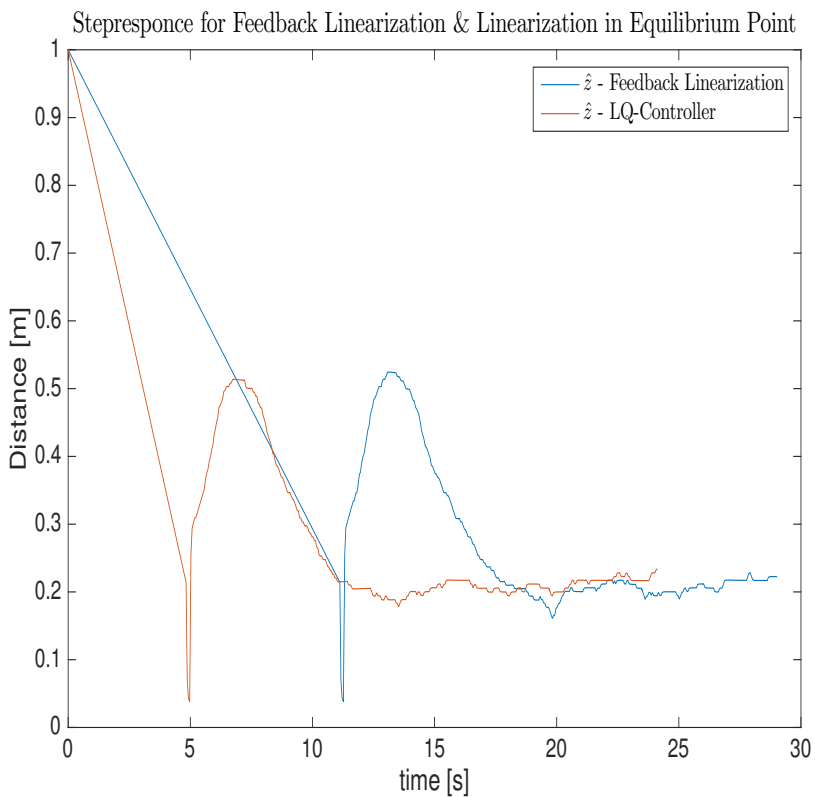


**Figure 6.6:** Illustrates a step response of two different controllers, feedback linearization and linearization in equilibrium point using LQ-controller. The step was taken from 1 [m] to 0.2 [m].

### 6.3.2 Trend-function

The algorithm using the trend function, Algorithm 1, was used in the simulation environment, both in Simulink and in Gazebo, with good results. The system model presented in Equation 4.10 was valid in the simulation environment and made the trend function method a valid tool to use when controlling the ALM. In reality, there are other outer characteristics that affect the outcome of the system. Example of such characteristics are uneven ground, altered friction, and measurement noise. This makes the trend function a bad alternative when navigating and controlling the ALM.

# 7

---

## Conclusions

This chapter contains a description of the conclusions reached in the thesis followed by a discussion of possible future work.

### 7.1 Conclusions

The conclusions of this thesis are that the navigation of the ALM using only one magnetic field sensor does not provide enough information to appropriately estimate the states of the system. This has effected the results when trying to control the system. The system model used in this thesis does not take in to consideration outer characteristics such as slip on the wheel, non-flat ground and measurement noise in the distance estimation. This results in large model estimation errors.

In simulations, the control strategy presented in this thesis works excellently, but the main challenge appears when controlling the real hardware outdoors. The control theory presented in this thesis has shown to be working when navigating along the magnetic loop at distances larger than 0.3 [m]. When navigating closer to the magnetic loop the uncertainties of the measurement causes the ALM to turn and wiggle its way forward in an unwanted way. These uncertainties of the distance are mainly caused by measurement noise and by wrongly determining the distance using the look-up table, seen as spikes in the estimates, represented by the blue line in the graphs presented in Figures 6.4 and 6.5.

Even if the reference distance is set to a distance larger than 0.3 [m], the ALM struggles in the curved parts of the magnetic loop track. The model used for the ALM during the tests preformed in this thesis does not contain a description of a curved loop. This will give a unwanted behavior such as overshoots in the corners. In the model presented in Equation 4.10 above, there are room for a

curved loop description in the function  $s_0$ . This function however can not be used in this thesis since there are no previous knowledge of the magnetic loop track. Moreover, the function  $s_0$  can only be estimated for a continuously shaped loop.

The implementation of the observer was a challenge since the measurement errors could not be modeled as white noise. There are other outer factors that affect the system that can not be explained in the system model or by modeling it as white noise. Since the theory for designing the weighting matrices does not hold the observer gain was estimated by evaluation of several tests. The one selected was the one with the best trade off in the manner of speed of following the measurements and robustness towards measurement noise.

When comparing the two control structures one could not by visual inspection tell which of the two that could followed the loop better than the other. Therefore when deciding which of the two control structures that is preferred it is more a matter of which would be least computational heavy. The least computational heavy would then be linearized in an equilibrium point model with an LQ-controller.

The result of this thesis was also affected by the fact that the magnetic field strength was filtered before treated in the algorithms presented in section 5.3.1 and 5.3.2. How much the pre-filtered signals affected the final results of this thesis is difficult to tell without performing new tests without filter.

## 7.2 Future work

For further work it is difficult to tell whether another control structure would give a better and more satisfying result than the ones evaluated in this thesis. One strategy that could be of interest to investigate is the Kalman filter with a prediction horizon. By using a Kalman filter with a prediction horizon the look-up table values might be chosen by the help of the observer estimations and not only by observing the derivative of the measurements. Another controller that might be of interest is an Model Predictive Controller (MPC). If an MPC were to be used, the saturation levels could be removed and the control signal could be optimized without exceeding the limit of the control signal.

Although there are many different control strategies that can be tested, the main issue for this navigation problem lies in the difficulties in measuring the distance to the magnetic loop.

# Appendix





# A

---

## Appendix A

---

### Algorithm 4 Altered saturation

---

```
1: procedure SATURATECONTROLSIGNAL( $\bar{z}, z_{ref}, u$ ) ▷
2:   Where  $\bar{z}$  is the control error,  $z_{ref}$  is the reference distance and  $u$  is the
   control signal.
3:   if  $\bar{z} < 0.1$  And  $0.2 < z_{ref} < 0.3$  And  $|u| > 0.15$  then
4:     if  $u > 0.15$  then
5:        $u = 0.15$ 
6:     else
7:        $u = -0.15$ 
8:     end if
9:   else if  $\bar{z} < 0.15$  And  $z_{ref} \leq 0.2$  And  $|u| > 0.15$  then
10:    if  $u > 0.15$  then
11:       $u = 0.15$ 
12:    else
13:       $u = -0.15$ 
14:    end if
15:  end if
16: end procedure
```

---



---

## Bibliography

- [1] M AICARDI. Closed loop steering of unicycle-like vehicles via lyapunov techniques. *IEEE Robotics Automat. Mag.*, pages 27–35, 1995. Cited on page 2.
- [2] David K. Cheng. *Field and Wave Electromagnetics*. Addison-Wesley Publishing Company, Inc, second edition, 1989. Cited on page 21.
- [3] Alessandro De Luca, Giuseppe Oriolo, and Claude Samson. Feedback control of a nonholonomic car-like robot. In *Robot motion planning and control*, pages 171–253. Springer, 1998. Cited on pages 2 and 14.
- [4] Rafael Fierro and Frank L Lewis. Control of a nonholonomic mobile robot: backstepping kinematics into dynamics. In *Decision and Control, 1995., Proceedings of the 34th IEEE Conference on*, volume 4, pages 3805–3810. IEEE, 1995. Cited on page 2.
- [5] L. Ljung G. Torkel. *Reglerteori, flervariabla och olinjära metoder*. Studentlitteratur, second edition, 2003. Cited on pages 5, 7, and 8.
- [6] Hassan K. Khalil. *Nonlinear systems*. Prentice Hall, Inc., third edition, 2002. Cited on page 5.
- [7] M. Vidyasagar Mark W. Spong, Seth Hutchinson. *ROBOT MODELING AND CONTROL*. John Wiley, Sons, Inc., second edition, 2006. Cited on page 10.
- [8] Alain Micaelli, Alain Micaelli, Claude Samson, Claude Samson, and Projet Icare. Trajectory tracking for unicycle-type and two-steering-wheels mobile robots, 1993. Cited on pages 2 and 14.
- [9] Angelo Morro, Antonio Sgorbissa, and Renato Zaccaria. Path following for unicycle robots with an arbitrary path curvature. *Robotics, IEEE Transactions on*, 27(5):1016–1023, 2011. Cited on page 2.
- [10] Chris Nielsen and Manfredi Maggiore. Maneuver regulation via transverse feedback linearization: Theory and examples. In *Proceedings of the IFAC symposium on nonlinear control systems (NOLCOS), Stuttgart, Germany*, pages 59–66, 2004. Cited on page 2.

- 
- [11] Christopher Nielsen, Cameron Fulford, and Manfredi Maggiore. Path following using transverse feedback linearization: Application to a maglev positioning system. *Automatica*, 46(3):585–590, 2010. Cited on page 2.
- [12] C Samson. Path followin and time-varyin feedback stabilization of a wheeled mobile robot\* p. 1992. Cited on pages 2 and 14.